ACS Medicinal Chemistry Letters

Design, Synthesis, and Evaluation of a New Chemotype Fluorescent Ligand for the P2Y₂ Receptor

Rebecca Knight, Laura E. Kilpatrick, Stephen J. Hill, and Michael J. Stocks*



Cite This: https://doi.org/10.1021/acsmedchemlett.4c00211



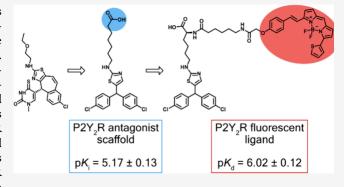
ACCESS I

Metrics & More

Article Recommendations

Supporting Information

ABSTRACT: The P2Y₂ receptor (P2Y₂R) is a target for diseases including cancer, idiopathic pulmonary fibrosis, and atherosclerosis. However, there are insufficient P2Y2R antagonists available for validating P2Y₂R function and future drug development. Evaluation of how (R)-5-(7-chloro-2-((2-ethoxyethyl)amino)-4Hbenzo[5,6]cyclohepta[1,2-d]thiazol-4-yl)-1-methyl-4-thioxo-3,4-dihydropyrimidin-2(1H)-one, a previously published thiazole-based analogue of AR-C118925, binds in a P2Y2R homology model was used to design new P2Y₂R antagonist scaffolds. One P2Y₂R antagonist scaffold retained millimolar affinity for the P2Y₂R and upon further functionalization with terminal carboxylic acid groups affinity was improved over 100-fold. This functionalized P2Y₂R antagonist scaffold was employed to develop new chemotype



P2Y₂R fluorescent ligands, that were attainable in a convergent five-step synthesis. One of these fluorescent ligands demonstrated micromolar affinity (p $K_d = 6.02 \pm 0.12$, n = 5) for the P2Y₂R in isolated cell membranes and distinct pharmacology from an existing P2Y₂R fluorescent antagonist, suggesting it may occupy a different binding site on the P2Y₂R.

KEYWORDS: Antagonists, Fluorescence, Ligands, Receptors

he P2Y receptors (P2YRs) are a family of eight G protein-coupled receptors (GPCRs), found in almost all cell and tissue types, which mediate the signaling of nucleotides.¹ The P2Y₂ receptor (P2Y₂R) is grouped with the "P2Y₁-like" receptors according to its sequence homology and primary coupling to Gq. 1 However, the P2Y2R is uniquely activated by both adenosine-5'-triphosphate (ATP) and uridine-5'-triphosphate (UTP) at equivalent concentrations. P2Y₂R signaling through G_q stimulates phospholipase C activity and the induction of the secondary messengers inositol-1,4,5-trisphosphate and diacylglycerol, which coordinate the release of Ca2+ ions from intracellular stores and activate protein kinase C, respectively.² The P2Y₂R is also coupled to the Go and G12 proteins, which activate Rac and Rho GTPases, and can signal through Src kinase.^{3–5}

Activation of the P2Y₂R has been identified as contributing to several clinical conditions. The P2Y₂R stimulated cytosolic phospholipase A2 and arachidonic acid release, which is subsequently metabolized to inflammatory molecules like prostaglandins, and are involved in diseases associated with chronic inflammation.⁶⁻⁹ In mouse models activation of the P2Y₂R induced vascular inflammation and atherosclerosis, with increased uptake of low-density lipoprotein in vascular smooth muscle. 10-12 While in mouse models of idiopathic pulmonary fibrosis P2Y2R deficiency reduced inflammation and fibrosis, preventing an ATP driven increase in macrophages and neutrophils, and migration of fibroblasts.¹³ In cancer, upon stimulation by ATP released from tumor cell-activated platelets, endothelial P2Y2R facilitated extravasation of tumor cells at metastatic sites by opening the endothelial barrier. ¹⁴ In several mouse models including breast and lung cancer, the knockout and/or pharmacological inhibition of the P2Y2R decreased tumor growth and reduced metastasis. 14-18 Despite being a promising therapeutic target, there is a lack of desirable P2Y₂R antagonists available for drug development or further pharmacological evaluation of P2Y₂R function and signaling.

AR-C118925 (1) is the most potent and selective antagonist for the P2Y2R, developed from UTP, with a midnanomolar IC₅₀ and 50- to 500-fold selectivity over other P2YR subtypes. 20,23 Despite being a helpful pharmacological tool, AR-C118925 had limited bioavailability when administered orally in preclinical studies, reflecting its poor physiochemical properties.²⁰ In a P2Y₂R homology model, docking studies suggested AR-C118925 bound in the orthosteric site and that occupation of a lipophilic binding pocket by the tricyclic 2,8dimethyl-5H-dibenzo[a,d][7]annulene group conferred high

Received: May 7, 2024 Revised: June 5, 2024 Accepted: June 10, 2024



receptor affinity and antagonist activity in calcium mobilization assays. 21,24 A series of AR-C118925 analogues have been detailed which replaced this moiety with 7-chloro-4*H*-benzo-[5,6] cyclohepta[1,2-d] thiazole to reduce lipophilicity. ¹⁹ The inclusion of linear, nonsterically demanding substituents on the thiazole ring increased affinity (for example compound 2) and provided a linking site for the attachment of fluorophores, generating the first fluorescent antagonist for the P2Y₂R with micromolar affinity (3) (Figure 1). ¹⁹ In bioluminescence

Figure 1. Illustrative structure for the thiazole-based series of $P2Y_2$ receptor antagonists (2), based on AR-C118925 (1), and the first fluorescent antagonist for the $P2Y_2$ receptor (3). 19,20

resonance energy transfer (BRET)-based assays, fluorescent antagonist 3 was used with P2Y₂R tagged on its *N*-terminus with NanoLuciferase (NLuc) to determine the affinities of several unlabeled P2Y₂R antagonists in NanoBRET competition binding experiments.¹⁹ Fluorescent antagonist 3 provides an indispensable tool to identify new P2Y₂R antagonists with the distance and orientation proximity required for Nano-BRET (10 nm) allowing determination of binding for low affinity compounds.^{19,25}

In the present study, the binding pose of **2**, a thiazole-based analogue of **1**, was evaluated in a $P2Y_2R$ homology model and used to design a new series of $P2Y_2R$ antagonist scaffolds. ^{19,21} Herein, we report the design, synthesis, and pharmacological evaluation of these $P2Y_2R$ antagonist scaffolds and their subsequent development into new chemotype fluorescent ligands that bind to the $P2Y_2R$ in membranes.

The synthetic strategy began with investigation of how **2**, the highest affinity compound in the thiazole-based series of P2Y₂R antagonists, might bind in a P2Y₂R homology model. ^{19,21} Induced-fit docking simulations for **2** demonstrated a different binding pose to **1**, with the thiouracil ring partially occupying the lipophilic binding pocket (Leu89, Phe113, Tyr114, Val168, Phe171, Val172, Phe195, and Phe261) and the thiazole substituent extended upward toward a basic amino acid triad (His184, Arg272, and Arg24) (Figure 2). ^{21,22} Interestingly, the tricyclic 7-chloro-4*H*-benzo[5,6]cyclohepta-[1,2-*d*]thiazole group is not anchored in the lipophilic binding pocket, despite these interactions being predicted as crucial for

the binding of 1 (p K_i = 7.38 \pm 0.04). The observed change in binding pose could result from steric constraints imposed by the linear thiazole substituent; more sterically demanding substituents were inactive at the P2Y₂R. Despite this different predicted binding pose, 2 retains good affinity for the P2Y₂R (p K_i = 6.56 \pm 0.16) which suggests replacement of the tricyclic ring system and thiouracil might be tolerated to generate a series of P2Y₂R antagonists with improved physiochemical properties. 19

To test this hypothesis, a series of potential P2Y₂R antagonists with sequential replacement of the tricyclic ring system and thiouracil were designed (Figure 3). Another predicted key interaction for the potency of 1, is the formation of ionic salt bridges between the acylated tetrazole, which would be deprotonated at physiological pH, and a basic amino acid triad (His184, Arg272, and Arg24) (Figure 2).²¹ In the binding pose of 2 the linear thiazole substituent 2-ethoxyethylamine extends upward toward the basic amino acid triad, and presents an opportunity to recapitulate the interactions of 1 with these amino acids through the incorporation of acidic groups. Thus, with an aim to improve affinity, any active P2Y₂R antagonist scaffolds would be functionalized with thiazole substituents containing terminal acidic groups (Figure 3).

The synthesis pathway to reach compounds 4-8 is shown in Scheme 1. The ethyl 2-chlorothiazole-4-carboxylate (10) and ethyl 2-chlorothiazole-5-carboxylate (17) were hydrolyzed to afford the carboxylic acids 11 and 18. Treatment of 11 and 18 with oxalyl chloride generated the acid chlorides, which were immediately converted to the Weinreb amides 12 and 19. The Weinreb amides were then reacted with Grignard reagent, 4chlorphenylmagnesium bromide, to provide the ketones 13 and 20 in a single addition. In the next step, 5-bromo-2,4-ditert-butoxypyrimidine was lithiated with n-butyllithium and then a 1,2-addition gave the tertiary alcohols 14 and 21. Subsequent deprotection and reduction was achieved with triethylsilane and trifluoracetic acid to give 15 and 22. Alkylation at the N-1 position with iodomethane in a onepot process that first involved reversible silylation of the carbonyl groups on the uracil, using N,O-bis(trimethylsilyl)trifluoroacetamide, was carried out to give 16 and 23. The thiazole chlorine atoms of 16 and 23 were displaced with 2ethoxyethylamine upon heating in the microwave under basic conditions to give 5 and 8. Finally, reaction with Lawesson's reagent provided the 4-thiouracils 4 and 7.

The synthesis pathway of compounds 6 and 9 is illustrated in Scheme 2. Compounds 10 and 17 were treated with excess Grignard reagent, 4-chlorophenylmagnesium bromide, to facilitate two step addition, to the ester and then ketone, formed through elimination, to give the tertiary alcohols 24 and 26. Subsequent reduction with triethylsilane and trifluoracetic acid afforded 25 and 27. The thiazole chlorine atoms of 25 and 27 were readily displaced with 2-ethoxyethylamine upon heating in the microwave under basic conditions to give 6 and 9.

These potential P2Y₂R antagonist scaffolds were then evaluated using NanoBRET to assess their ability to displace fluorescent antagonist 3, and consequently reduce the BRET ratio, at a single antagonist point concentration of 100 μ M (Table 1). These experiments were performed in membrane preparations made from clonal 1321N1 cells stably expressing the NLuc tagged P2Y₂R. Of the new P2Y₂R antagonist scaffolds only compound 9 significantly reduced the BRET

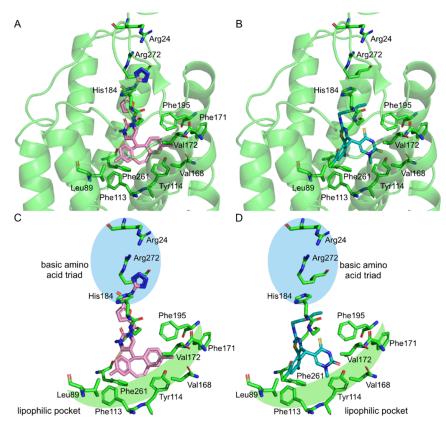


Figure 2. Putative binding pose of AR-C118925 (A + C) and thiazole-based analogue 2 (B + D) in a published homology model of the $P2Y_2$ receptor with important residues in the binding pocket shown.²¹ The receptor is shown in cartoon representation, while amino acids (green), AR-C118925 (pink), and 2 (teal) are displayed as stick models. Oxygen atoms are shown in red, nitrogen in blue, chlorine in green, and sulfur in yellow. Docking experiments were performed using OEDocking Hybrid Docking.²² Homology model kindly supplied by Dr Müller.²¹

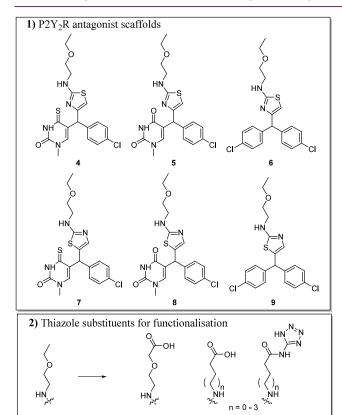


Figure 3. Structure of potential P2Y₂R antagonists.

ratio (** P < 0.01 one-way ANOVA with Tukey's multiple comparison test). Interestingly compound **6**, the regioisomer of **9**, demonstrated no reduction of the BRET ratio suggesting that the position of the thiazole ring is important for retaining binding. This could reflect either the formation of a key interaction with the thiazole group or a conformational preference for one regioisomer. However, **9** was not soluble at the higher concentrations required to complete a dose–response competition binding assay. We estimate that compound **9** had a $pKi = \sim 3$ because the BRET ratio could be reduced by 44% at 1 mM (Supplementary Figure 1).

With the aim to increase the affinity of scaffold 9 through engagement of the potential P2Y₂R basic amino acid triad (His184, Arg272, and Arg24) previously identified (Figure 2), a new series of P2Y₂R antagonists with thiazole substituents containing terminal acidic groups were synthesized (Scheme 3). These included amino acids with varying carbon chain lengths to probe the distance required to engage the basic amino acid triad and incorporation of the tetrazole group which increased affinity ~10-fold in the development of 1.¹⁹

The preparation of these compounds is detailed in Scheme 3. The thiazole chlorine atom of 27 was displaced with a range of amines through nucleophilic aromatic substitution upon heating in the microwave under basic conditions to give compounds 28-33. Subsequent activation with benzotriazol-1-yl-oxytripyrrolidinophosphonium hexafluorophosphate and reaction with 5-aminotetrazole was then only tolerated by compound 33 to afford the tetrazole 34.

Compounds 28-34 were then evaluated using NanoBRET to assess their ability to displace 3 from NLuc-P2Y₂R in 1321N1

Scheme 1. Synthesis of Compounds 4-23^a

"Reagents and conditions: (a) NaOH, THF/H₂O, rt, overnight (98%). (b) (i) Oxalyl chloride, catalytic DMF, THF, rt, 5 h (ii) DIPEA, *N,O*-dimethylhydroxylamine-HCl, DCM, rt, overnight (99% over two steps). (c) 4-Chlorophenylmagnesium bromide, THF, -78 °C to rt, overnight (40–62%). (d) (i) 5-Bromo-2,4-di-*tert*-butoxypyrimidine, *n*-butyllithium, THF, -78 °C, 15 min; (ii) **14**, -78 °C to rt, 1 h (17–55%). (e) TFA, triethylsilane, DCM, rt, 30 min (16–71%). (f) (i) *N,O*-Bis(trimethylsilyl)trifluoroacetamide, 1,2-dichloroethane, reflux, 18 h; (ii) iodomethane, 50 °C, 18 h (62%). (g) 2-Ethoxyethylamine, triethylamine, DMSO, 150 °C, 30 min (26–45%). (h) Lawesson's reagent, 1,4-dioxane, reflux, 18 h (4–43%).

Scheme 2. Synthesis of Compounds $6-27^a$

"Reagents and conditions: (a) 4-Chlorophenylmagnesium bromide, THF, -78 °C to rt, overnight (58–63%). (b) TFA, triethylsilane, DCM, rt, 30 min (82–84%). (c) 2-Ethoxyethylamine, triethylamine, DMSO, 150 °C, 30 min (53–57%).

cell membrane preparations, with their pK_i values reported in Table 1. The inclusion of the carboxylic acid group increased affinity, with pK_i values that could now be determined in the low micromolar range. Concurrently, protecting the carboxylic acid group with an ester, as in 31, caused a dramatic drop in activity. Compound 29, with the (2-aminoethoxy)acetic acid group analogous to 2, did not demonstrate significantly improved affinity compared to 30 (P > 0.05 one-way ANOVA with Tukey's multiple comparison test) which had the same carbon chain length; suggesting the ethoxy group is

Table 1. Affinities for New P2Y2 Receptor Antagonists

Compound	$pK_i \pm (SEM)^a/\%$ BRET signal inhibition at 100 μ M ^b	% calcium mobilization inhibition at 10 μM^d
4	$IA^{c}(3)$	-
5	4% (3)	-
6	IA (3)	-
7	2% (3)	-
8	IA (3)	-
9	32% (3)	-
28	$4.49 \pm 0.07 (4)$	20% (3)
29	$4.71 \pm 0.06 (3)$	18% (3)
30	$4.87 \pm 0.02 (3)$	16% (3)
31	12% (3)	-
32	$4.84 \pm 0.10 (3)$	14% (3)
33	$5.17 \pm 0.13 (4)$	19% (3)
34	$5.04 \pm 0.10 (3)$	5% (3)

^aThe estimated affinity values (pK_i) for each antagonist in NanoBRET competition binding experiments with 2 μM of fluorescent antagonist 3. ^bPercentage inhibition of BRET signal with 2 μM of 3 and 100 μM of a test compound. ^cIA = inactive; i.e., no inhibition of BRET signal at 100 μM. The pK_i and percentage inhibition of BRET signal experiments were carried out in membrane preparations of 1321N1 astrocytoma cells clonally expressing recombinant NanoLuc-P2Y₂R. The final concentration of DMSO was <10%. ^dPercentage inhibition of calcium mobilization induced by P2Y₂R agonist UTPγS at 100 nM in 1321N1 astrocytoma cells expressing P2Y₂R when treated with 10 μM of a test compound. The final concentration of DMSO was 1%. For all experiments, data points are mean values, and where appropriate ± SEM, with the number of separate experiments given in parentheses and performed in triplicate observations.

Scheme 3. Synthesis of Compounds 28-34

"Reagents and conditions: (a) NH_2R , DIPEA, DMSO, 120 °C, 2–12 h (4–56%). (b) 5-Aminotetrazole monohydrate, DIPEA, PyBroP, DMF, rt, overnight (9%).

not making a specific interaction with the P2Y₂R. Compound 30 had a significantly higher affinity than 28 (*** P < 0.001 one-way ANOVA with Tukey's multiple comparison test), indicating that the length of the carbon chain is important for positioning the carboxylic acid group. Although not statistically significant, there was a trend for increased affinity with the presence of a longer carbon chain. Compound 33 displayed the highest affinity of the series ($pK_i = 5.17 \pm 0.13$) which is at least a 100-fold increase on compound 9 ($pK_i = \sim 3$). However, conversion of the carboxylic acid to the tetrazole in the case of 34 did not reproduce the improvement in affinity previously demonstrated for 1.²⁰ These results support the hypothesis that functionalization of the new P2Y₂ antagonist

scaffold 9 with thiazole substituents containing terminal acidic groups increases affinity through interactions with the $P2Y_2R$.

We then sought to determine whether these functionalized $P2Y_2R$ antagonist scaffolds retained their ability to inhibit calcium mobilization induced by the $P2Y_2R$ agonist UTP γ S in $P2Y_2R$ expressing 1321N1 cells. Compounds 28-34 were tested at 10 μ M but were not fully soluble at the highest percentage of DMSO that can be tolerated by living cells. At this single point concentration of 10 μ M, compounds 28–34 demonstrated minimal inhibition of calcium mobilization, which reflects their low affinity and insolubility (Table 1). This demonstrates the utility of NanoBRET based assays which, due to their high sensitivity, can be used to identify and monitor the binding of low affinity compounds, that offer starting points for future optimization and structure—activity relationship elucidation. ²⁵

These new P2Y2R antagonist scaffolds were then used to develop a series of fluorescent ligands for the P2Y2R which can be obtained in fewer synthetic steps than 3 (a 17-step synthesis with <1% overall yield). 19 The strategy involved the incorporation of the amino acids ornithine and lysine into the P2Y₂R antagonist scaffold, as they retain the carboxylic acid group that was crucial for affinity while the amine provides a functional handle for attachment of fluorophores. The choice of fluorophore can significantly impact the affinity and properties of a fluorescent ligand. Previous studies have demonstrated that fluorescent ligands incorporating watersoluble fluorophores, such as Alexa Fluor and sulfonated cyanine dyes, exhibit reduced affinity compared to their counterparts containing more lipophilic BODIPY and TAMRA dyes. 26-28 These differences in affinity have been attributed to the more lipophilic fluorophores favoring association with the receptor, rather than the extracellular medium, thus presenting an opportunity to engage key residues.^{27,28} Therefore, because our P2Y2R antagonist scaffolds exhibited low affinity we chose to incorporate the fluorophores BODIPY 630/650-X, BODIPY FL-X, and 5-TAMRA as an opportunity to further improve affinity.

The preparation of these compounds is detailed in Scheme 4. The thiazole chlorine atom of 27 was displaced with Boc-Orn-OtBu or Boc-Lys-OH upon heating in the microwave under basic conditions to yield 35 and 40, respectively. The Boc and OtBu protecting groups were then removed and the amine conjugated to the commercially available fluorophores BODIPY 630/650-X, BODIPY FL-X, and 5-TAMRA to give six fluorescent ligands (37-40 and 42-44) in good yields. These fluorescent ligands were then evaluated using Nano-BRET saturation binding assays in membrane preparations from NLuc-P2Y₂R 1321N1 cells.

All fluorescent ligands demonstrated some degree of specific binding, with the nonspecific component defined using a high concentration of 33 (Figure 4). However, the BODIPY FL-X containing compounds 38 and 43 had elevated levels of nonspecific binding, that could reflect the promiscuous association of these lipophilic fluorescent ligands with the membrane in close enough proximity to the NLuc-P2Y₂R so that bystander BRET can still occur. Low levels of saturable nonspecific binding were also seen for the BODIPY 630/650-X and 5-TAMRA containing compounds 37, 39, 42, and 44, which suggests these fluorescent ligands also associate with the membrane surrounding the NLuc-P2Y₂R but to a lesser extent. Therefore, to determine the affinity of these fluorescent ligands the nonspecific binding component was deducted from total

Scheme 4. Synthesis of Compounds 35-44^a

"Reagents and conditions: (a) NHR $_1$ R $_2$ DIPEA, DMSO, 120 °C, 1 h (21%–61%) (b) TFA, DCM, 1 h, quantitative (c) BODIPY630/650–X-NHS, BODIPYFL-X-NHS or 5-TAMRA NHS ester, DIPEA, DMF, 1–4 h (25–97%).

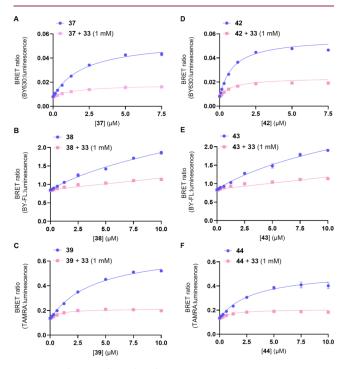


Figure 4. Pharmacological evaluation using NanoBRET in saturation binding assays for (A) 37, (B) 38, (C) 39, (D) 42, (E) 43, and (F) 44 with the absence or presence of $P2Y_2R$ antagonist 33 at 1 mM, to determine the nonspecific binding component, in membrane preparations of 1321N1 astrocytoma cells clonally expressing recombinant NanoLuc- $P2Y_2R$. The data points are the mean values of each experiment \pm SEM (n=3, except for 42 which is n=5) and performed in triplicate observations.

binding and pK_d values derived where saturable specific binding was observed (Table 2).

Table 2. NanoBRET Affinities for P2Y₂ Receptor Fluorescent Ligands 37-39 and 42-44

Compound	$pK_d \pm (SEM)^a$
37	$5.64 \pm 0.07 (3)$
38	ND^b
39	ND
42	$6.02 \pm 0.12 (5)$
43	ND
44	5.38 ± 0.19 (3)

^aThe estimated affinity value (p K_d) for each fluorescent ligand was measured in NanoBRET saturation binding curves in membrane preparations of 1321N1 astrocytoma cells clonally expressing recombinant NanoLuc-P2Y₂R. ^bND = not determined, i.e., not determined because binding did not saturate at 10 μM. Data points are mean values \pm SEM from the number of separate experiments given in parentheses and performed in triplicate observations.

Only compounds 37, 42 and 44 demonstrated saturable specific binding (Figure 5). For both scaffolds the BODIPY 630/650-X containing ligands 37 and 42 had the highest affinity and increased affinity compared to 33, demonstrating

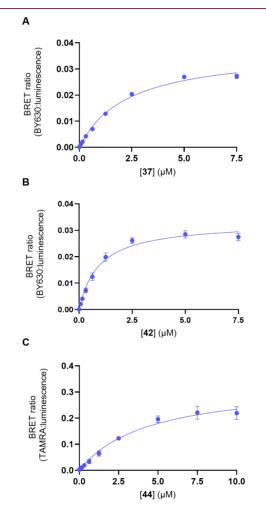


Figure 5. Specific binding component from NanoBRET saturation binding assays for (A) 37, (B) 42, and (C) 44 with the nonspecific binding component, defined with P2Y₂R antagonist 33 at 1 mM, deducted in membrane preparations of 1321N1 astrocytoma cells clonally expressing recombinant NanoLuc-P2Y₂R. The data points are the mean values of each experiment \pm SEM (n = 3, except for 42 which is n = 5) and performed in triplicate observations.

the ability of the fluorophore to engage with key residues in the $P2Y_2R$ that contribute to an improved affinity, and is consistent with previous studies. There was no significant difference between the affinities of 37 and 42 (P > 0.05 oneway ANOVA with Tukey's multiple comparison test). However, since 44 demonstrated saturable specific binding and 39 did not, the length of the carbon chain did impact affinity of the 5-TAMRA containing fluorescent ligands.

Compound 42 had the highest affinity of all the fluorescent ligands in the micromolar range (p K_d = 6.02 \pm 0.12) and a good window between the specific and nonspecific binding components. NanoBRET saturation binding assays were also carried out for compound 42 in NLuc-CXCR4 expressing HEK293 cell membrane preparations to investigate the contribution of bystander BRET and potential off-target effects (Supplementary Figure 2). The BRET signal for 42 in NLuc-CXCR₄ membranes was minimal and predominantly displaceable by 33, which suggests 42 is binding to endogenous P2Y₂R in close enough proximity to NLuc-CXCR4 that bystander BRET can still occur (Supplementary Figure 2). Although not a measure of selectivity, the minimal BRET signal observed in NLuc-CXCR₄ membranes suggests that 42 is specifically binding to the P2Y₂R in these experiments. However, we are not able to comment on the selectivity of 42 across other P2Y receptor family members because of its low affinity and the lack of selective fluorescent ligands available for the other P2Y family members that would allow low affinity compounds to be evaluated. The affinity of fluorescent ligand 42 was also assessed using the NanoBRET competition binding assay with 3 in NLuc-P2Y₂R membrane preparations from 1321N1 cells (Figure 6). The affinity of 42 from the NanoBRET

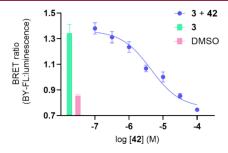


Figure 6. NanoBRET competition binding assay of **42** with 2 μ M of fluorescent antagonist 3 in membrane preparations of 1321N1 astrocytoma cells clonally expressing recombinant NanoLuc-P2Y₂R. The data points are the mean values of each experiment \pm SEM (n=5) and performed in triplicate observations.

competition binding assay (p K_i = 5.48 \pm 0.30) was not significantly different from the affinity measured through the NanoBRET saturation binding assay (p K_i = 6.02 \pm 0.12) (P > 0.05 unpaired t test), with complete displacement of 3 observed in a concentration-dependent manner (Figure 6).

To evaluate the utility of the new fluorescent ligand 42 we then performed NanoBRET competition binding assays with literature compound 1, our highest affinity new P2Y₂R antagonist 33, and the *N*-Boc-protected precursor for 42, compound 40 (Figure 7 and Table 3). The affinity of 1 estimated from competition binding with 42 was significantly lower (** P < 0.01 unpaired t test), with an over 1,000-fold difference, to the value determine with 3. The affinity of compound 40 determined with 3 and 42 was also significantly different (* P < 0.05 unpaired t test), again with 42 predicting

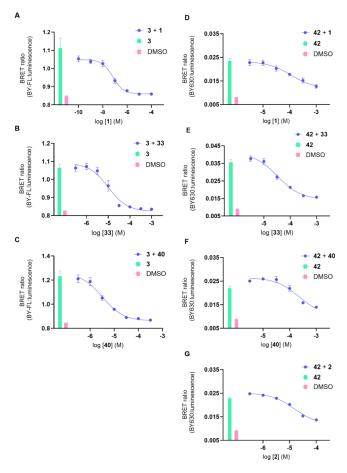


Figure 7. NanoBRET competition binding assays with fluorescent ligands 3 and 42 in membrane preparations of 1321N1 astrocytoma cells clonally expressing recombinant NanoLuc-P2Y₂R. Specifically, competition binding of 1 with (A) 3 (2 μ M), (D) 42 (0.75 μ M); 33 with (B) 3 (2 μ M), (E) 42 (1.5 μ M); and 40 with either (C) 3 (2 μ M) or (F) 42 (0.75 μ M). The data points are the mean values of each experiment \pm SEM (n = 3 for experiments with 3 and n = 5 for experiments with 42).

Table 3. Comparison of Affinity Estimates for P2Y₂ Receptor Antagonists Obtained from Competition with the Binding of Fluorescent Ligand 3 or 42

Compound	$pK_i \pm (SEM)$ with 3^a	$pK_i \pm (SEM)$ with 42^a
1	$7.49 \pm 0.28 (3)$	$4.14 \pm 0.07 (5)$
2	$6.56 \pm 0.16 (3)^{b}$	$5.04 \pm 0.06 (5)$
33	$5.17 \pm 0.13 (4)$	$4.86 \pm 0.05 (5)$
40	$5.61 \pm 0.01 (3)$	$3.92 \pm 0.14 (5)$
42	$5.48 \pm 0.30 (5)$	$6.02 \pm 0.12 (5)^{c}$

^aThe estimated affinity value (p K_i) for each antagonist was measured in NanoBRET competition binding experiments with fluorescent ligands 3 (2 μM) and 42 (0.75 μM for 1, 2 and 40, 1.5 μM for 33). ^bValue taken from literature. ¹⁹ ^cThe estimated affinity value (p K_d) for 42 measured from NanoBRET saturation binding curves. All experiments were carried out in membrane preparations of 1321N1 astrocytoma cells clonally expressing recombinant NanoLuc-P2Y₂R. Data points are mean values \pm SEM from the number of separate experiments given in parentheses and performed in triplicate observations.

a lower affinity. The affinity of compound 2 estimated with 42 was also lower than previously determined with 3. However, there was no significant difference between the affinities

determined for compound 33 when using 3 or 42 as the fluorescent ligand (P > 0.05 unpaired t test). These results suggest that fluorescent ligand 42 might not occupy the same binding site on the $P2Y_2R$ to its precursor 40, AR-C118925, and 2 but can still influence their binding, along with new $P2Y_2R$ antagonist scaffold 33 and fluorescent antagonist 3.

In conclusion, through evaluation of the binding pose of 2 in a P2Y₂R homology model we have designed and identified the P2Y₂R antagonist scaffold 9, which without the tricycle ring or thiouracil retained weak affinity (p $K_i = \sim 3$) for the P2Y₂R in membranes. Subsequent functionalization of this P2Y₂R antagonist scaffold with terminal carboxylic acid groups, to promote proposed engagement with a basic amino acid triad located in the P2Y₂R binding site, improved affinity at least 100-fold in the case of compound 33 (p $K_i = 5.17 \pm 0.13$). Compound 33 offers a starting point for further optimization to develop new P2Y₂R antagonists and elucidate structure activity relationships.

This P2Y₂R antagonist scaffold was then employed to develop a new series of P2Y₂R fluorescent ligands, that were attainable in a convergent five-step synthesis. Fluorescent ligand 42 demonstrated micromolar affinity (p K_d = 6.02 \pm 0.12) for the P2Y₂R in membranes and distinct pharmacology from 3 in NanoBRET competition binding assays, which suggest it occupies a different binding site on the P2Y₂R. The novel properties of fluorescent ligand 42 should expand the toolbox of ligands available to study the P2Y₂R.

ASSOCIATED CONTENT

Data Availability Statement

The data that support the findings of this study are available from the corresponding author upon reasonable request.

Supporting Information

The Supporting Information is available free of charge at https://pubs.acs.org/doi/10.1021/acsmedchemlett.4c00211.

Percentage inhibition of BRET signal by compound 9, NanoBRET saturation binding for fluorescent ligand 42 in NLuc-CXCR₄ membrane preparations, chemistry methods, and pharmacology methods (PDF)

AUTHOR INFORMATION

Corresponding Author

Michael J. Stocks — Division of Biomolecular Sciences and Medicinal Chemistry, School of Pharmacy, University of Nottingham, Nottingham NG7 2RD, U.K.; orcid.org/0000-0003-3046-137X; Phone: +44 (0)115951 5151; Email: michael.stocks@nottingham.ac.uk

Authors

Rebecca Knight — Division of Biomolecular Sciences and Medicinal Chemistry, School of Pharmacy, University of Nottingham, Nottingham NG7 2RD, U.K.; Centre of Membrane Proteins and Receptors (COMPARE), Universities of Birmingham and Nottingham, The Midlands NG7 2UH, U.K.; orcid.org/0000-0001-8344-654X

Laura E. Kilpatrick — Division of Biomolecular Sciences and Medicinal Chemistry, School of Pharmacy, University of Nottingham, Nottingham NG7 2RD, U.K.; Centre of Membrane Proteins and Receptors (COMPARE), Universities of Birmingham and Nottingham, The Midlands NG7 2UH, U.K.; orcid.org/0000-0001-6331-5606

Stephen J. Hill — Centre of Membrane Proteins and Receptors (COMPARE), Universities of Birmingham and Nottingham, The Midlands NG7 2UH, U.K.; Division of Physiology, Pharmacology and Neuroscience, School of Life Sciences, University of Nottingham, Nottingham NG7 2UH, U.K.; orcid.org/0000-0002-4424-239X

Complete contact information is available at: https://pubs.acs.org/10.1021/acsmedchemlett.4c00211

Author Contributions

The project was conceived by M.J.S., S.J.H., and L.E.K. Experiments were designed by all authors and carried out by R.K. The manuscript was written through contributions of all authors. All authors have given approval to the final version of the manuscript.

Notes

The authors declare no competing financial interest.

ACKNOWLEDGMENTS

This work was supported by a Wellcome Trust PhD studentship [218466/Z/19/Z] to RK and the Medical Research Council UK [grant number MR/W023768/1]. L.E.K was supported by a University of Nottingham Anne McLaren Fellowship.

ABBREVIATIONS

ANOVA, analysis of variance; ATP, adenosine-5'-triphosphate; BODIPY, boron-dipyrromethene; BRET, bioluminescence resonance energy transfer; CXCR₄, C-X-C chemokine receptor type 4; DMSO, dimethyl sulfoxide; GPCRs, G protein-coupled receptors; IC₅₀, half-maximal inhibitory concentration; K_d , dissociation constant of a labeled ligand—receptor complex; K_i , dissociation constant of a ligand—receptor complex determined through a binding assay; NLuc, nanoluciferase; SEM, standard error of the mean; 5-TAMRA, 5-carboxytetrame-thylrhodamine; UTP, uridine-5'-triphosphate; UTP γ S, uridine-5'-(γ -thio)-triphosphate

REFERENCES

- (1) Jacobson, K. A.; Delicado, E. G.; Gachet, C.; Kennedy, C.; Kügelgen, I.; Li, B.; Miras-Portugal, M. T.; Novak, I.; Schöneberg, T.; Perez-Sen, R.; Thor, D.; Wu, B.; Yang, Z.; Müller, C. E. Update of P2Y receptor pharmacology: IUPHAR Review 27. *Br. J. Pharmacol.* 2020, 177 (11), 2413–2433.
- (2) Abbracchio, M. P.; Burnstock, G.; Boeynaems, J.-M.; Barnard, E. A.; Boyer, J. L.; Kennedy, C.; Knight, G. E.; Fumagalli, M.; Gachet, C.; Jacobson, K. A.; Weisman, G. A. International Union of Pharmacology LVIII: Update on the P2Y G Protein-Coupled Nucleotide Receptors: From Molecular Mechanisms and Pathophysiology to Therapy. *Pharmacol. Rev.* **2006**, *58* (3), 281–341.
- (3) Bagchi, S.; Liao, Z.; Gonzalez, F. A.; Chorna, N. E.; Seye, C. I.; Weisman, G. A.; Erb, L. The P2Y2Nucleotide Receptor Interacts with αvIntegrins to Activate Goand Induce Cell Migration. *J. Biol. Chem.* **2005**, 280 (47), 39050–39057.
- (4) Liao, Z.; Seye, C. I.; Weisman, G. A.; Erb, L. The P2Y2 nucleotide receptor requires interaction with v integrins to access and activate G12. *Journal of Cell Science* **2007**, *120* (9), 1654–1662.
- (5) Liu, J.; Liao, Z.; Camden, J.; Griffin, K. D.; Garrad, R. C.; Santiago-Pérez, L. I.; González, F. A.; Seye, C. I.; Weisman, G. A.; Erb, L. Src Homology 3 Binding Sites in the P2Y2 Nucleotide Receptor Interact with Src and Regulate Activities of Src, Proline-rich Tyrosine Kinase 2, and Growth Factor Receptors. *J. Biol. Chem.* **2004**, 279 (9), 8212–8218.

- (6) Xu, J.; Weng, Y. I.; Simonyi, A.; Krugh, B. W.; Liao, Z.; Weisman, G. A.; Sun, G. Y. Role of PKC and MAPK in cytosolic PLA2 phosphorylation and arachadonic acid release in primary murine astrocytes. *J. Neurochem* **2002**, *83* (2), 259–70.
- (7) Xu, J.; Chalimoniuk, M.; Shu, Y.; Simonyi, A.; Sun, A. Y.; Gonzalez, F. A.; Weisman, G. A.; Wood, W. G.; Sun, G. Y. Prostaglandin E2 production in astrocytes: regulation by cytokines, extracellular ATP, and oxidative agents. *Prostaglandins Leukot Essent Fatty Acids* **2003**, *69* (6), 437–48.
- (8) Xing, M.; Post, S.; Ostrom, R. S.; Samardzija, M.; Insel, P. A. Inhibition of phospholipase A2-mediated arachidonic acid release by cyclic AMP defines a negative feedback loop for P2Y receptor activation in Madin-Darby canine kidney D1 cells. *J. Biol. Chem.* **1999**, 274 (15), 10035–8.
- (9) Welch, B. D.; Carlson, N. G.; Shi, H.; Myatt, L.; Kishore, B. K. P2Y2 receptor-stimulated release of prostaglandin E2 by rat inner medullary collecting duct preparations. *Am. J. Physiol Renal Physiol* **2003**, 285 (4), F711–21.
- (10) Chen, X.; Qian, S.; Hoggatt, A.; Tang, H.; Hacker, T. A.; Obukhov, A. G.; Herring, P. B.; Seye, C. I. Endothelial Cell-Specific Deletion of P2Y2 Receptor Promotes Plaque Stability in Atherosclerosis-Susceptible ApoE-Null Mice. *Arterioscler Thromb Vasc Biol.* **2017**, *37* (1), 75–83.
- (11) Stachon, P.; Geis, S.; Peikert, A.; Heidenreich, A.; Michel, N. A.; Unal, F.; Hoppe, N.; Dufner, B.; Schulte, L.; Marchini, T.; Cicko, S.; Ayata, K.; Zech, A.; Wolf, D.; Hilgendorf, I.; Willecke, F.; Reinohl, J.; von Zur Muhlen, C.; Bode, C.; Idzko, M.; Zirlik, A. Extracellular ATP Induces Vascular Inflammation and Atherosclerosis via Purinergic Receptor Y2 in Mice. *Arterioscler Thromb Vasc Biol.* **2016**, *36* (8), 1577–86.
- (12) Dissmore, T.; Seye, C. I.; Medeiros, D. M.; Weisman, G. A.; Bradford, B.; Mamedova, L. The P2Y2 receptor mediates uptake of matrix-retained and aggregated low density lipoprotein in primary vascular smooth muscle cells. *Atherosclerosis* **2016**, 252, 128–135.
- (13) Muller, T.; Fay, S.; Vieira, R. P.; Karmouty-Quintana, H.; Cicko, S.; Ayata, K.; Zissel, G.; Goldmann, T.; Lungarella, G.; Ferrari, D.; Di Virgilio, F.; Robaye, B.; Boeynaems, J. M.; Blackburn, M. R.; Idzko, M. The purinergic receptor subtype P2Y2 mediates chemotaxis of neutrophils and fibroblasts in fibrotic lung disease. *Oncotarget* 2017, 8 (22), 35962–35972.
- (14) Schumacher, D.; Strilic, B.; Kishor; Wettschureck, N.; Offermanns, S. Platelet-Derived Nucleotides Promote Tumor-Cell Transendothelial Migration and Metastasis via P2Y2 Receptor. *Cancer Cell* **2013**, *24* (1), 130–137.
- (15) Woods, L. T.; Jasmer, K. J.; Munoz Forti, K.; Shanbhag, V. C.; Camden, J. M.; Erb, L.; Petris, M. J.; Weisman, G. A. P2Y2 receptors mediate nucleotide-induced EGFR phosphorylation and stimulate proliferation and tumorigenesis of head and neck squamous cell carcinoma cell lines. *Oral Oncol* **2020**, *109*, No. 104808.
- (16) Jin, H.; Eun, S. Y.; Lee, J. S.; Park, S. W.; Lee, J. H.; Chang, K. C.; Kim, H. J. P2Y2 receptor activation by nucleotides released from highly metastatic breast cancer cells increases tumor growth and invasion via crosstalk with endothelial cells. *Breast Cancer Res.* **2014**, *16* (5), R77.
- (17) Li, W. H.; Qiu, Y.; Zhang, H. Q.; Liu, Y.; You, J. F.; Tian, X. X.; Fang, W. G. P2Y2 receptor promotes cell invasion and metastasis in prostate cancer cells. *Br. J. Cancer* **2013**, *109* (6), 1666–75.
- (18) Hu, L. P.; Zhang, X. X.; Jiang, S. H.; Tao, L. Y.; Li, Q.; Zhu, L. L.; Yang, M. W.; Huo, Y. M.; Jiang, Y. S.; Tian, G. A.; Cao, X. Y.; Zhang, Y. L.; Yang, Q.; Yang, X. M.; Wang, Y. H.; Li, J.; Xiao, G. G.; Sun, Y. W.; Zhang, Z. G. Targeting Purinergic Receptor P2Y2 Prevents the Growth of Pancreatic Ductal Adenocarcinoma by Inhibiting Cancer Cell Glycolysis. *Clin. Cancer Res.* **2019**, 25 (4), 1318–1330.
- (19) Conroy, S.; Kindon, N. D.; Glenn, J.; Stoddart, L. A.; Lewis, R. J.; Hill, S. J.; Kellam, B.; Stocks, M. J. Synthesis and Evaluation of the First Fluorescent Antagonists of the Human P2Y2 Receptor Based on AR-C118925. *J. Med. Chem.* **2018**, *61* (7), 3089–3113.

- (20) Kindon, N.; Davis, A.; Dougall, I.; Dixon, J.; Johnson, T.; Walters, I.; Thom, S.; McKechnie, K.; Meghani, P.; Stocks, M. J. From UTP to AR-C118925, the discovery of a potent non nucleotide antagonist of the P2Y2 receptor. *Bioorg. Med. Chem. Lett.* **2017**, 27 (21), 4849–4853.
- (21) Rafehi, M.; Neumann, A.; Baqi, Y.; Malik, E. M.; Wiese, M.; Namasivayam, V.; Müller, C. E. Molecular Recognition of Agonists and Antagonists by the Nucleotide-Activated G Protein-Coupled P2Y2 Receptor. J. Med. Chem. 2017, 60 (20), 8425–8440.
- (22) McGann, M. FRED and HYBRID docking performance on standardized datasets. J. Comput. Aided Mol. Des 2012, 26 (8), 897–906.
- (23) Rafehi, M.; Burbiel, J. C.; Attah, I. Y.; Abdelrahman, A.; Müller, C. E. Synthesis, characterization, and in vitro evaluation of the selective P2Y2 receptor antagonist AR-C118925. *Purinergic Signalling* **2017**, *13* (1), 89–103.
- (24) Neumann, A.; Attah, I.; Al-Hroub, H.; Namasivayam, V.; Muller, C. E. Discovery of P2Y2 Receptor Antagonist Scaffolds through Virtual High-Throughput Screening. *J. Chem. Inf Model* **2022**, 62 (6), 1538–1549.
- (25) Stoddart, L. A.; Kilpatrick, L. E.; Hill, S. J. NanoBRET Approaches to Study Ligand Binding to GPCRs and RTKs. *Trends Pharmacol. Sci.* **2018**, 39 (2), 136–147.
- (26) Vernall, A. J.; Stoddart, L. A.; Briddon, S. J.; Hill, S. J.; Kellam, B. Highly potent and selective fluorescent antagonists of the human adenosine A(3) receptor based on the 1,2,4-triazolo[4,3-a]quinoxalin-1-one scaffold. *J. Med. Chem.* **2012**, *55* (4), 1771–82.
- (27) Comeo, E.; Kindon, N. D.; Soave, M.; Stoddart, L. A.; Kilpatrick, L. E.; Scammells, P. J.; Hill, S. J.; Kellam, B. Subtype-Selective Fluorescent Ligands as Pharmacological Research Tools for the Human Adenosine A(2A) Receptor. *J. Med. Chem.* **2020**, *63* (5), 2656–2672.
- (28) Comeo, E.; Trinh, P.; Nguyen, A. T.; Nowell, C. J.; Kindon, N. D.; Soave, M.; Stoddart, L. A.; White, J. M.; Hill, S. J.; Kellam, B.; Halls, M. L.; May, L. T.; Scammells, P. J. Development and Application of Subtype-Selective Fluorescent Antagonists for the Study of the Human Adenosine A(1) Receptor in Living Cells. *J. Med. Chem.* **2021**, *64* (10), 6670–6695.
- (29) Kok, Z. Y.; Stoddart, L. A.; Mistry, S. J.; Mocking, T. A. M.; Vischer, H. F.; Leurs, R.; Hill, S. J.; Mistry, S. N.; Kellam, B. Optimization of Peptide Linker-Based Fluorescent Ligands for the Histamine H(1) Receptor. *J. Med. Chem.* **2022**, *65* (12), 8258–8288.